Title
Sex-dependent long-term effects of prepubescent stress on the posterior parietal cortex

Authors
Fariborzi, Mona
Bin Park, Soo
Ozgur, Ali
et al.

Publication Date
2021-05-01

DOI
10.1016/j.ynstr.2021.100295

Peer reviewed

Neurobiology of Stress 14 (2021) 100295

Contents lists available at ScienceDirect

Neurobiology of Stress

journal homepage: www.elsevier.com/locate/ynstr

Sex-dependent long-term effects of prepubescent stress on the posterior parietal cortex

Mona Fariborzi, Soo Bin Park, Ali Ozgur, Gyorgy Lur *

Department of Neurobiology and Behavior, University of California, 1215 McGaugh Hall, Irvine, CA, 92697, USA

ARTICLE INFO

Keywords:
Adolescent stress
Sex differences
Long-term effects
Parietal cortex
Excitatory
Inhibitory synapses

ABSTRACT

Adolescence is a time of intense cortical development and a period of heightened sensitivity to insult. To determine how sex affects the short- and long-term outcomes of early-adolescent stress exposure, we subjected prepubescent (postnatal day 30) male and female mice to repeated multiple concurrent stressors (RMS). In the posterior parietal cortex (PPC), RMS caused the elimination of excitatory synapses in deeper layers while inhibitory synapse density was predominantly diminished in superficial layers. These short-term effects coincided with reduced visuo-spatial working memory and were similar in both sexes. The loss of excitatory synapses and impaired working memory persisted in males past a 30-day recovery period. In contrast, we observed a remarkable recovery of excitatory transmission and behavioral performance in females. Inhibitory synapse density recovered in both sexes. We have also observed a late onset anxiety phenotype in RMS exposed females that was absent in males. Overall, our results indicate that there are marked sex differences in the long-term effects of prepubescent stress on cortical synapses and behavior.

1. Introduction

Adolescence is a period of intense brain development in humans (Blakemore and Choudhury, 2006; Giedd and Rapoport, 2010; Lenroot and Giedd, 2006) and rodents (Mengler et al., 2014; Spear, 2000; Zoratto et al., 2018) alike. Since the central nervous system is primed for change during this time, adolescent stress exposure can have an exaggerated impact (Romeo et al., 2006; Andersen, 2003; Dahl, 2004). In human subjects, childhood adversity leads to measurable negative effects later in life. For example, abuse occurring up to the age of 16 was associated with weak academic performance (Boden et al., 2007), and reduced visual memory, executive functioning, and spatial working memory (Gould et al., 2012) in adulthood. Although there is mounting evidence that adolescent stress has a marked impact on cognitive function in mice and rats (Eiland and Romeo, 2013; Romeo, 2013), rodent models of this age group remain surprisingly understudied.

The first report on the effect of chronic stress in adolescent rodents showed arrested hippocampal development and weakened spatial memory performance in male rats (Isgor et al., 2004). Following studies showed reduced dendritic complexity in the prefrontal cortex (Eiland et al., 2012), diminished inhibition but unchanged excitation in superficial layers (Ito et al., 2010), and weakened glutamatergic transmission in deep cortical layers (Yuen et al., 2012). These experiments focused on specific structures or synapse types, making comparisons across studies difficult. Repeated exposure to stress in adolescence also resulted in reduced spatial memory (Sterlemann et al., 2010), impaired fear memory (Ito et al., 2010), diminished temporal order recognition memory (Yuen et al., 2012), or depression like behavioral phenotypes (Eiland et al., 2012). In adult rodents the impact of repeated stress was frequently found to be reversible (Conrad et al., 1999; Luine et al., 1994; McEwen, 1999; Radley et al., 2005). Yet, multiple time point studies of adolescent stress affects are rare (Isgor et al., 2004; Leussis et al., 2008).

Sex differences in stress response are well-documented both in humans and animal models (Bangasser and Wiersielis, 2018; Beck and Luine, 2002; Conrad et al., 2003; Kitraki et al., 2004; Luine et al., 2017; Ortiz et al., 2015). However, studies comparing the effect of adolescent stress in males and females are relatively scarce. Chronic restraint during adolescence similarly affected dendritic length in both sexes in the hippocampus, prefrontal cortex and the amygdala (Eiland et al., 2012). Chronic unpredictable stress also resulted in similar behavioral effects in adolescent males and females (Yohn and Blendy, 2017). Conversely, repeated social stress in adolescent rats was shown to induce sex-specific changes in intrinsic excitability, glutamatergic transmission and dendritic structure in the prefrontal cortex (Urban et al., 2019; Urban and

* Corresponding author.
E-mail address: glur@uci.edu (G. Lur).

https://doi.org/10.1016/j.ynstr.2021.100295
Received 21 October 2020; Received in revised form 3 January 2021; Accepted 4 January 2021
Available online 13 January 2021

Valentino, 2017). A similar pattern emerges regarding stress-induced cognitive deficits: restraint stress affected working memory performance similarly in males and females (Conrad et al., 2003; Shansky et al., 2006) while repeated social stress induced sex-specific changes (Snyder, 2015; Snyder et al., 2015). Differences in stress response are likely due to a complex interaction of multiple factors, including sex differences in corticosterone release (Kitay, 1961), the sensitivity to corticotropin releasing factor (CRF) (Salvatore et al., 2018; Bangasser et al., 2010), and orexins (Grafe et al., 2017) as well as the impact of gonadal hormones like estrogen (McEwen, 2014; McEwen and Milner, 2007).

Stress-induced cognitive deficits are frequently linked to alterations in the synaptic architecture (Magarinos and McEwen, 1995; Radley et al., 2006; Sousa et al., 2000), and functional connectivity (Liston et al., 2006, 2009; Soares et al., 2012) of the hippocampus or the prefrontal cortex (PFC). However, there is growing evidence that the parietal circuit is also affected by stress. Functional imaging revealed altered parietal metabolism in combat veterans (Bremner et al., 1999a), trauma victims (Piefke et al., 2007), and women with a history of abuse (Bremner et al., 1999b, 2004; Lanius et al., 2002). A disruption of parietal functional connectivity is a reoccurring observation in subjects repeatedly exposed to psychosocial stress or traumatic events like war, torture, or childhood abuse (Liston et al., 2009; Dunkley et al., 2015; Hart et al., 2017; Kolassa et al., 2007). Underpinning this stress-sensitivity, parietal regions were found to be rich in CRF receptors in mice (Chen et al., 2000) and corticosteroid receptors both in rodents (Stark et al., 1975) and primates (Sanchez et al., 2000). While the role of the parietal lobe in cognitive functions has been long appreciated (Shomstein, 2012), our understanding of how stress affects this region at the synaptic level is very limited.

We have previously shown that repeated exposure to multiple concurrent stressors (RMS for short) during the prepubescent period has a marked impact on excitatory synapses in the posterior parietal cortex (PPC). We causally linked this synapse loss to impaired performance in spontaneous alternation in the Y-maze, a test of visuo-spatial working memory (Libovner et al., 2020). The current study had two objectives: (1) determine the effects of RMS on excitatory and inhibitory synaptic transmission in the PPC and on the associated cognitive performance and (2) unveil the influence of sex on the short- and long-term impact of prepubescent RMS. To this end, we exposed male and female mice to 10 days of RMS starting at postnatal day 30, followed by histology and electrophysiology measurements. We quantified excitatory and inhibitory synaptic transmission in the PPC immediately after RMS and after a 30-day recovery period. We tested the effect of RMS on visuo-spatial working memory as well as learned helplessness and anxiety behaviors. We found that the immediate impact of prepubescent RMS was similar in males and females but marked sex differences emerged following the recovery period.

2. Materials and methods

2.1. Animals

All experiments were performed in accordance with the NIH guidelines on the care and use of laboratory animals and approved by the Institutional Animal Care and Use Committee (AUP-17-145). C57BL/6J mice were either purchased from Charles River (~10% of the animals used in the study) or bred in house. Purchased mice arrived in our facility at age p23 and spent approximately one week acclimating. Mice bred in house were weaned at p21 and equal numbers of littermates were randomly assigned to control or stress conditions. All animals were group-housed in a quiet, uncrowded facility on a 12 h light/dark cycle, with ad libitum access to lab chow and water.

2.2. Stress paradigm

On postnatal day 30 (p30), mice were assigned to one of the following groups: repeated exposure to multiple concurrent stressors (RMS), stress free control, RMS + 30-day rest, stress free control + 30-day rest. RMS animals were exposed to multiple concurrent stressors for 1 h a day for 10 consecutive days (Libovner et al., 2020; Hokenson et al., 2020; Chen et al., 2008; Maras et al., 2014). Briefly, mice were restrained in well ventilated 50 ml conical tubes and 5 to 8 of them were placed in a clean cage. The cage was on a laboratory rocker to jostle the tubes. An LED provided flashing lights, and a high frequency speaker connected to an audio amplifier and an Arduino Uno delivered a loud noise stimulus (for details see (Hokenson et al., 2020)). Experiments were carried out 2 h after the last stress session.

The 30-day rest cohorts underwent the same stress paradigm followed by a 30-day recovery period during which animals were left undisturbed in their home cages. Mice were used for behavioral tests or sacrificed for histology or electrophysiology at p70.

2.3. Immunohistochemistry

Age matched control and RMS mice were transcardially perfused with phosphate buffered saline (PBS) followed by 4% paraformaldehyde (PFA) dissolved in Sorenson's buffer and postfixed for 5 h in 4% PFA. Then, 50 μm coronal slices were prepared from the posterior parietal region on a vibrating microtome (Compresstome 300z). From the mouse PPC this yielded 8–10 sections. We assigned 4 of these slices to examine excitatory synapses and another 4 to the study of inhibitory synapses. Slice selection was interleaved to efficiently sample the entire PPC in the two staining conditions. Slices were washed in Sorenson's buffer, and nonspecific staining was blocked for 1 h at room temperature with 10% normal goat serum (NGS), 1% bovine serum albumin (BSA) and 0.1% Triton X-100 dissolved in Sorenson's buffer. After blocking, slices were transferred to a staining solution with 5% NGS, 1% BSA, and anti-postsynaptic density-95 (PSD-95) monoclonal antibody (7E3–1B8, Thermo Fisher Scientific) at 1:1500 dilution or anti-Gephyrin (Synaptic Systems, 147 021) at 1:1000 dilution in Sorenson's buffer for overnight staining at 4 °C on a laboratory shaker. Slices were then washed four times in Sorenson's buffer and transferred into a secondary antibody solution which contained anti-mouse secondary antibody conjugated to Alexa Fluor 555 (1:500) for 2 h. Following four washes in Sorenson's buffer, slices were mounted on microscope slides with Prolong Diamond anti-fade reagent with DAPI and covered with a no. 1 thickness cover glass.

2.4. Confocal microscopy

PSD-95 and Gephyrin staining was visualized on an LSM 700 Confocal Microscope (Zeiss) in the University of California, Irvine, Optical Biology Core using a 63 × oil-immersion objective. Hippocampal images were taken as 5 × 5 tiles at 1 × optical zoom (0.2 μm pixel size) to include all layers of the dorsal hippocampus. PPC images were 3 × 10 tiles at 1 × optical zoom to include the entire cortical column. All images were collected 10 μm below the slice surface to ensure identical antibody penetration between experiments. The PPC was imaged at 1300–1500 μm from the midline. Alexa Fluor 555 was excited at 555 nm. Fluorescence emissions were separated using a 500 nm beam splitter and filtered with a 560 nm long-pass filter.

2.5. Quantification of synapses

Synaptic density was automatically evaluated in CellProfiler (Lamprecht et al., 2007; McQuin et al., 2018) as described before (Libovner et al., 2020). To avoid experimenter biases, all conditions (control and RMS) were loaded together, and the analysis was run on this combined batch of images. To count PSD-95 and Gephyrin puncta in

specific layers of hippocampus and PPC, 100 μm^2 subsections were randomly cropped from visually identified layers and automatically assigned into their respective groups based on metadata extracted from the image files. PSD-95 and Gephyrin puncta were detected via an object identification algorithm (Libovner et al., 2020). Synaptic density was then given as the number of puncta per 100 μm^2 of brain tissue.

2.6. Behavioral tests

Behavioral tests were conducted directly after 10 days of RMS, and 30 days after the last RMS session. To minimize the potentially confounding effects of behavioral testing we employed the following strategy: mice were first tested in the Y-maze or Light/Dark box (LDB) test with half of the mice starting in the Y-maze followed by LDB and the other half tested in the opposite order. After completing these two experiments, mice were either exposed to forced swim (2/3 of animals) or to sucrose preference (remaining 1/3). Sucrose preference experiments were discontinued when the lack of stress effect became clear. Animals were subjected to no more than three of the four tests. Furthermore, only half of the mice used in immunostaining or electrophysiology experiments were exposed to any behavioral testing at all. Behaviors were either scored using automated software or by two independent investigators who were blind to the animals' condition if manual scoring was necessary.

2.7. Y-maze

To measure spontaneous alternation, we used a standard Y-maze apparatus (350 mm long arms at 120° angles). Large geometrical shapes were displayed outside of the maze at easily visible angles to serve as visual cues. Control and stressed animals were placed into a randomly selected arm of the maze, and their behavior was captured on video at 30 frames/s for 8 min. Video footage was analyzed using batch processing in Camlytics software and spontaneous alternations were calculated as follows: spontaneous alternation (%) = (number of spontaneous alternations/total number of arm entries −2) * 100 (Miedel et al., 2017) using a custom script written in Python 3.7 (Anaconda).

2.8. Light/dark box

We used a homemade light/dark box that consisted of a mouse cage partitioned with a laminated cardboard wall with one third spray painted to opacity. The wall had a small opening to allow transit between the chambers. The overall dimensions of the light dark box were 8 × 13 inches, with the dark side being 8 × 4 inches and the light side being 8 × 9 inches. Activity in the box was filmed with a webcam (Logitech) positioned above the box. Mice were placed in the dark portion and left to explore for 6 min. Videos of control and RMS mice were simultaneously processed by automated image analysis software (Camlytics), and the resulting data was analyzed via custom scripts in Python 3.7.

2.9. Forced swim test

Mice were placed in a glass cylinder filled with water (23 ± 1 °C) and their behavior was recorded for 6 min on a webcam. Time to the first bout of immobility ("latency to immobile") and the total time spent immobile in the last 4 min of the videos were scored by two independent investigators both of whom were blinded to the condition of the animal. After scoring, results between the two observers were averaged.

2.10. Sucrose preference test

A subgroup of mice was moved to individual cages with a 12 h light/dark cycle, with ad libitum access to lab chow for approximately 24 h. During this time, two bottles were available, one with water and one with 3% sucrose water. After 12 h the bottles were switched to control for positional preferences. The bottles were weighed before and after the 24 h period. Sucrose preference was expressed as (amount of sucrose water consumed)/(amount of total liquid consumed) * 100.

2.11. Electrophysiology

All electrophysiology measurements were obtained from age matched control and stressed mice. When possible a control and a stressed animal was recorded on the same day using the same solutions. Under isoflurane anesthesia mice were transcardially perfused with warm (30–32 °C (Ankri et al., 2014)) cutting solution containing (in mM): 110 choline, 25 NaHCO3, 1.25 NaH2PO4, 3 KCl, 7 MgCl2, 0.5 CaCl2, 10 glucose, 11.6 sodium ascorbate and 3.1 sodium pyruvate, bubbled with 95% O2 and 5% CO2. 300 μm thick slices containing the PPC were prepared on a Z-deflection calibrated vibrating blade microtome (Campden smz 7000-2, Lafayette Instruments) and maintained in the cutting solution for an additional 15 min at 32 °C (Ting et al., 2014). After incubation, slices were transferred to artificial cerebrospinal solution (ACSF) containing (in mM): 126 NaCl, 26 NaHCO3, 1.25 NaH2PO4, 3 KCl, 1 MgCl2, 2 CaCl2, 10 glucose, bubbled with 95% O2 and 5% CO2 in a holding chamber at room temperature and maintained for 20–30 min before use.

All experiments were conducted close to physiological temperature (32–34 °C) in a submersion type recording chamber mounted on an Olympus BX51-WI microscope. Whole-cell patch-clamp recordings were obtained from Layer 2/3 (150–250 μm from the pia surface) or layer 5 pyramidal cells (300–500 μm from the pia surface) identified with video-infrared/differential interference contrast. For voltage-clamp recordings, glass electrodes (2–4 MΩ) were filled with internal solution containing (in mM): 135 CsMeSO3, 10 HEPES, 4 MgCl2, 4 Na2ATP, 0.4 NaGTP, 10 sodium creatine phosphate, and adjusted to pH 7.3 with CsOH. Series resistance was 9–16 MΩ, recordings outside of this range were discarded. Electrophysiological recordings were made using a MultiClamp 700B amplifier (Molecular Devices), filtered at 3 kHz, and digitized at 20 kHz. Data was acquired using National Instruments DAQ boards and Wavesurfer software written in Matlab (HHMI Janelia Research Campus). To capture miniature synaptic events the slice was bathed in 3 μM TTX (Tocris) for at least 5 min. From each cell we recorded 5 min at −70mV holding potential to capture excitatory events (mEPSCs) then another 5 min at 0 mV membrane potential to record inhibitory events (mIPSCs).

Offline analysis was performed using custom routines in Matlab. Briefly, we developed a graphical user interface that implemented a template matching algorithm based on Clements and Bekkers (1997). We used a stringent detection criterion of 5 to identify synaptic events. Our software is freely available for download at https://github.com/gyorgylur/MiniAnalysis.

2.12. Chemicals

All salts and chemical used in this study were from Sigma unless otherwise specified.

2.13. Statistical analysis

All histology, behavior, an electrophysiology data collection was performed in parallel in age-matched control and stressed animals with the experimenter blinded to the condition of the animal. To avoid batch effects every experiment was conducted on several cohorts. In histology experiments, we imaged three to four brain slices per animal (see Methods/Immunohistochemistry for details). Synaptic puncta counts from these slices were then averaged and a single value per animal was used for statistical comparisons; thus, the degrees of freedom (*n* numbers) for every experiment represent individual animals. For slice physiology, we typically recorded 2–4 cells per animal. Data from the

same cell type was averaged to give us one data point per cell type per animal, thus the degrees of freedom (*n* numbers) for slice physiology experiments are also individual animals. Statistical comparisons between two independent groups were made using Student's t-test. When more than two groups were compared, we used one-way ANOVA tests and results were corrected for multiple comparisons using Bonferroni's method. To test for sex differences in the effect of stress, we used two-way ANOVA with post hoc comparisons between groups. These post hoc tests were corrected for multiple comparisons using Bonferroni's method.

3. Results

3.1. RMS-induced loss of deep-layer excitatory synapses only persists in males

Using PSD95 immunostaining (Fig. 1A), we have previously shown that prepubescent exposure to RMS leads to a marked loss of excitatory synapses from the deeper layers of the PPC and from the hippocampus (Libovner et al., 2020). We have reproduced these results ($p_{L1} = 0.32$, $p_{L2/3} > 1$, $p_{L5} = 0.0068$, $p_{L6} = 0.039$, n = 6, one-way ANOVA, Bonferroni's correction, Fig. 1B) and found the same pattern of cortical synapse loss in females immediately following RMS exposure ($p_{L1} > 1$, $p_{L2/3} > 1$, $p_{L5} = 0.0078$, $p_{L6} = 0.026$, n = 8, one-way ANOVA, Bonferroni's correction, Fig. 1C). Two-way ANOVA revealed significant main effects for stress ($F_{1, 21} = 17.71$, p = 0.0004) and sex ($F_{1, 21} = 5.966$, p = 0.0231) in deep cortical layers. After correcting for multiple comparisons, we found significant sex difference in control (p = 0.04) but not in RMS mice (p = 0.34) and significant stress effect in males (p = 0.026) and in females (p = 0.0003). Interestingly, unlike in males, RMS did not result in hippocampal synapse loss in females (males: $p_{SR} = 0.017$, n = 6, females: $p_{SR} = 0.4$, n = 8, *t*-test, Fig. 1C) and two-way ANOVA revealed significant main effect for sex ($F_{1, 21} = 6.103$, p = 0.022) with a marked difference in the RMS condition (p = 0.032). Following the 30-day recovery period, synapse loss persisted in deep cortical layers and the hippocampus of males when compared to age matched controls ($p_{L1} = 0.14$, $p_{L2/3} > 1$, $p_{L5} = 0.036$, $p_{L6} = 0.039$, n = 6, one-way ANOVA, Bonferroni's correction, $p_{SR} = 0.039$, n = 6, *t*-test, Fig. 1D). Conversely, synapse numbers in females were indistinguishable between control and RMS exposed mice in all cortical layers and the hippocampus after 30 days of rest (all p-values > 0.7, n = 10, one-way ANOVA, Bonferroni's correction, $p_{SR} = 0.32$, n = 10, *t*-test, Fig. 1E). Two-way ANOVA revealed significant main effect for sex ($F_{1, 31} = 7.807$, p = 0.0086). Post hoc analysis found significant sex difference in RMS mice (p = 0.0006) but not in control (p > 0.99). Sex differences persisted in hippocampal synapse density (main sex effect: $F_{1, 31} = 7.831$, p = 0.009).

To confirm that RMS-induced loss of PSD95 puncta corresponds to fewer excitatory synapses we made whole cell voltage clamp recordings from layer 2/3 and layer 5 pyramidal neurons in the PPC. Action potential firing in the slice was blocked with tetrodotoxin, allowing us to measure spontaneous release "miniature" synaptic events. Miniature excitatory postsynaptic currents (mEPSCs) were recorded with the neuron's membrane potential clamped at −70mV (Fig. 2A and D). In layer 2/3 pyramidal neurons we did not detect a difference in the frequency of mEPSCs at either time point in either of the sexes (males: $p_{L2/3, 0d} = 0.37$, n = 5, $p_{L2/3, 30d} = 0.26$, n = 5, females: $p_{L2/3, 0d} = 0.42$, n = 6, $p_{L2/3, 30d} = 0.76$, n = 5, *t*-test, Fig. 2B and C). In males we observed a slight decrease in the amplitude of layer 2/3 mEPSCs immediately after RMS ($p_{L2/3, 0d} = 0.0055$, n = 5, *t*-test, Fig. 2B) which recovered after 30 days of rest ($p_{L2/3, 30d} = 0.4$, n = 5, *t*-test, Fig. 2B). We did not observe an RMS effect on amplitude in females (p > 0.4 at both time points, *t*-test, Fig. 2C). In layer 5 pyramidal neurons of male mice, we detected a robust decrease in mEPSC frequency immediately after RMS that persisted after the 30-day rest period ($p_{L5, 0d} = 0.0023$, n = 5, $p_{L5, 30d} = 0.0004$, n = 6, *t*-test, Fig. 2E). In females, we saw reduced mEPSC frequency in layer 5 pyramidal neurons immediately after RMS that returned to control level after 30 days of rest ($p_{L5, 0d} = 0.035$, n = 6, $p_{L5, 30d} = 0.3$, n = 5, *t*-test, Fig. 2F). Two-way ANOVA indicated significant main effect for stress ($F_{1, 19} = 18.97$, p = 0.0003) as well as sex ($F_{1, 19} = 9.120$, p = 0.0070) immediately after RMS. Post hoc analysis revealed significant sex difference in control (p = 0.028) but not in the RMS condition (p = 0.26). Following the 30-day rest period, we found significant main effect for stress ($F_{1, 18} = 12.91$, p = 0.0021) and significant stress × sex interaction ($F_{1,18} = 7.911$, p = 0.012). Correcting for

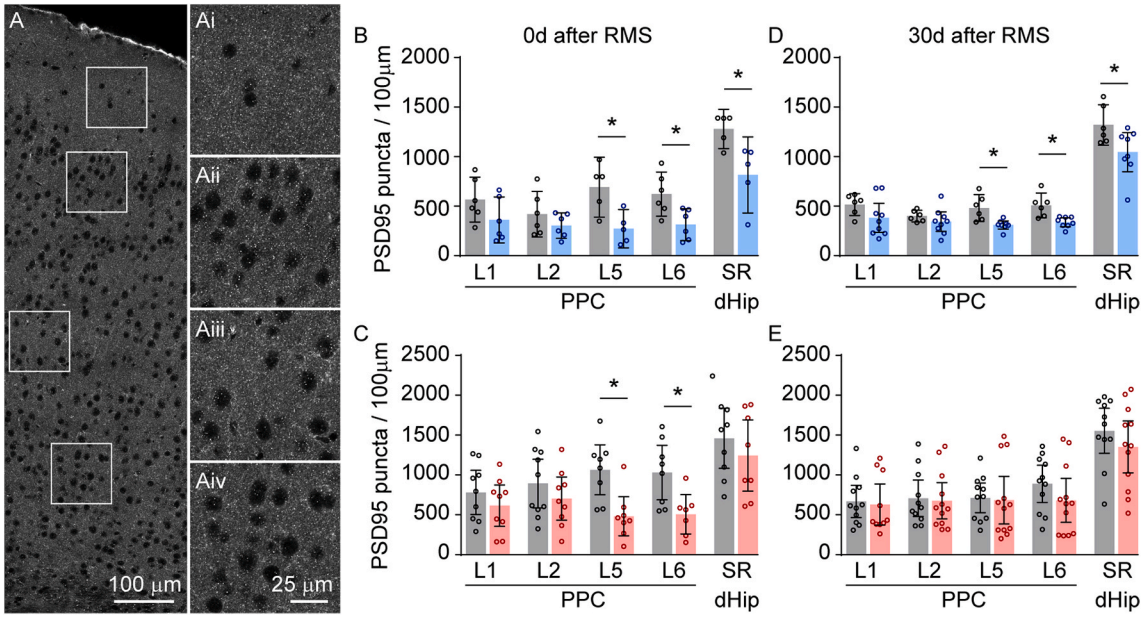

Fig. 1. RMS induces persistent loss of PSD95 puncta in deep layers of the PPC in males. (**A**) Example florescent image of PSD95 staining in the PPC with insets showing example 100 µm crops from cortical layers 1, 2/3, 5 and 6. PSD95 puncta density in control (gray) and immediately after RMS in (**B**) males (blue) and (**C**) females (red) in layers 1, 2/3, 5, and 6 of the PPC and the stratum radiatum (SR) of the dorsal hippocampus (dHip). PSD95 puncta density following the 30-day rest period control (gray) in RMS exposed (**D**) males (blue) and (**E**) females (red). All bars represent mean with 95% confidence intervals, *: p < 0.05. (For interpretation of the references to colour in this figure legend, the reader is referred to the Web version of this article.)

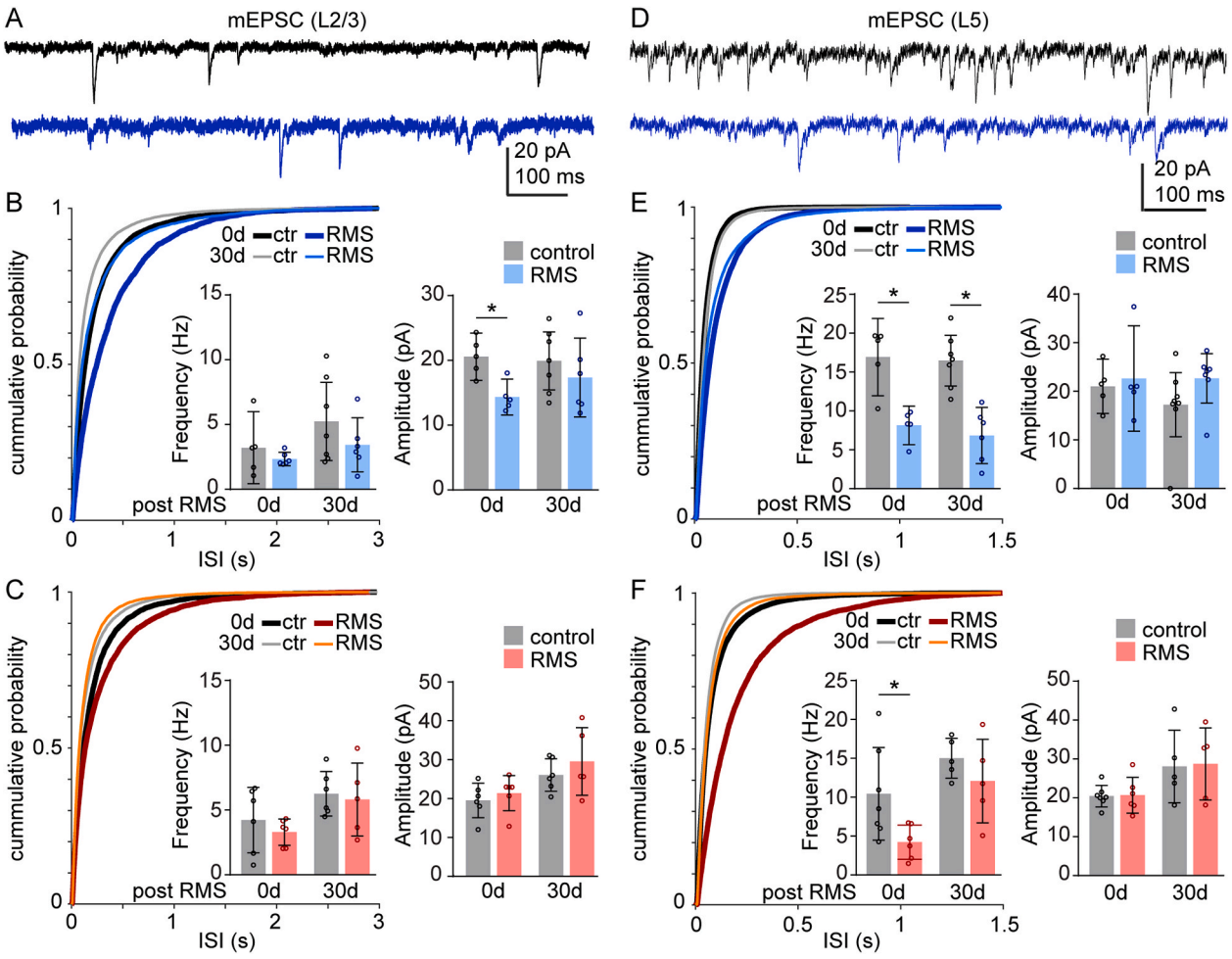

Fig. 2. RMS induces persistent decrease of miniature EPSC frequency in layer 5 pyramidal neurons in males. (**A**) Example miniature EPSC (mEPSC) recordings from layer 2/3 pyramidal neurons in the PPC of control (black) and RMS exposed (blue) mice. mESPC frequency and amplitude in layer 2/3 pyramidal neurons in control (gray) and post-RMS in (**B**) males (blue) and (**C**) females (red). (**D**) Example miniature EPSC (mEPSC) recordings from layer 5 pyramidal neurons in the PPC of control (black) and RMS exposed (blue) mice. mESPC frequency and amplitude in layer 5 pyramidal neurons in control (gray) and post-RMS in (**E**) males (blue) and (**F**) females (red). All bars represent mean with 95% confidence intervals, *: $p < 0.05$. RMS induces temporary loss of superficial layer inhibitory synapses in both sexes. (For interpretation of the references to colour in this figure legend, the reader is referred to the Web version of this article.)

multiple comparisons revealed significant sex differences in RMS ($p = 0.011$) but not in control ($p = 0.96$) and significant stress effect in males ($p = 0.0002$) but not in females ($p > 0.99$). We did not measure a change in mEPSC amplitude in either sex at either time point (males: $p_{L5,\ 0d} = 0.72$, $n = 5$, $p_{L5,\ 30d} = 0.15$, $n = 6$; females: $p_{L5,\ 0d} = 0.9$, $n = 6$, $p_{L5,\ 30d} = 0.91$, $n = 5$, *t*-test Fig. 2E and F).

Our electrophysiology measurements match our histology observations, indicating a persistent, RMS-induced loss of excitatory synapses from deeper cortical layers in male mice while excitatory synapses in RMS-exposed females show a remarkable recovery after 30 days.

Inhibition is a critical part of the cortical synaptic architecture, yet data on the effects of adolescent stress on inhibitory synapses is scarce. To determine the effect of RMS on inhibition in the cortex and hippocampus, we immunostained the postsynaptic inhibitory scaffolding protein Gephyrin (Fig. 3A). In male mice, we found a marked reduction in the density of Gephyrin puncta in cortical layers 1, 2/3 and 5 as well as the hippocampus immediately after RMS ($p_{L1} = 0.0014$, $p_{L2/3} = 0.01$, $p_{L5} = 0.004$, $p_{L6} = 0.14$, $n = 7$, one-way ANOVA, Bonferroni's correction, $p_{SR} = 0.013$, $n = 7$, *t*-test, Fig. 3B). Conversely, in females, RMS only reduced inhibitory Gephyrin staining in layers 1 and 2/3; puncta density in deeper layers and the hippocampus was indistinguishable from control ($p_{L1} = 0.017$, $p_{L2/3} = 0.037$, $p_{L5} = 0.47$, $p_{L6} > 1$, $n = 8$, one-way ANOVA, Bonferroni's correction, $p_{SR} = 0.68$, $n = 8$, *t*-test, Fig. 3C). In superficial cortical layers, two-way ANOVA revealed significant main effect for stress ($F_{1,\ 26} = 18.96$, $p = 0.0002$) but not for sex ($F_{1,\ 26} = 2.258$, $p = 0.1450$), while post hoc comparisons found no sex difference in control ($p = 0.21$) or RMS ($p > 0.99$) but significant stress effect in both males ($p = 0.0028$) and females ($p = 0.034$). In the hippocampus we found significant stress × sex interaction ($F_{1,\ 26} = 10.98$, $p = 0.0027$) immediately after RMS with detectable sex difference in RMS mice ($p = 0.02$) but not in control ($p = 0.14$) and significant stress effect in males ($p = 0.01$) but not in females ($p > 0.99$). Following the 30-day recovery period, we only detected reduced Gephyrin puncta density in the hippocampus of male mice ($p_{SR} = 0.0057$, $n = 14$, *t*-test; Fig. 3D) where two-way ANOVA revealed significant stress effect ($F_{1,\ 41} = 11.27$, $p = 0.0017$) and post hoc analysis indicated sex differences in RMS mice ($p = 0.02$) but not in controls ($p = 0.14$). Post-recovery, inhibitory synapse numbers in the PPC of males and all examined areas of female mice appeared similar between RMS and control animals (males: all p-values in PPC > 0.9, on-way ANOVA, Bonferroni's correction, $n = 14$, females: all p-values in PPC > 0.7, one-way ANOVA, Bonferroni's correction, $n = 10$, $p_{SR} = 0.062$, $n = 10$, *t*-test, Fig. 3D and E). Two-way ANOVA revealed no main stress or sex effects ($F_{1,\ 37} < 0.75$, $p > 0.3$ for all cases) on cortical Gephyrin puncta densities after the recovery period.

To test whether Gephyrin immunostaining results accurately represented functional inhibitory synapses in the PPC, we made whole cell

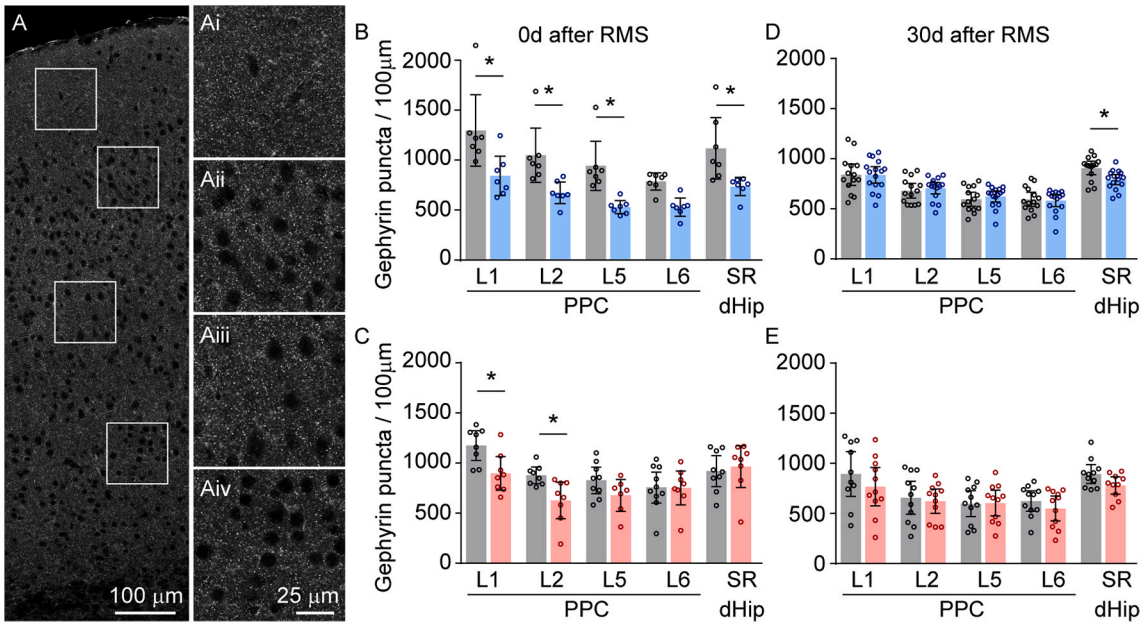

Fig. 3. RMS induces transient loss of gephyrin staining in superficial layers of the PPC in both sexes. (**A**) Example florescent image of Gephyrin staining in the PPC with insets showing example 100 µm crops from cortical layers 1, 2/3, 5 and 6. Gephyrin puncta density in control (gray) and immediately after RMS in (**B**) males (blue) and (**C**) females (red) in layers 1, 2/3, 5, and 6 of the PPC and the stratum radiatum (SR) of the dorsal hippocampus (dHip). Gephyrin puncta density following a 30-day rest period control (gray) in RMS exposed (**D**) males (blue) and (**E**) females (red). All bars represent mean with 95% confidence intervals, *: $p < 0.05$. (For interpretation of the references to colour in this figure legend, the reader is referred to the Web version of this article.)

voltage clamp recordings from layer 2/3 and layer 5 pyramidal neurons. Miniature inhibitory postsynaptic currents (mIPSCs) were measured with the neuron's membrane potential clamped at 0 mV (Fig. 4A, D). In layer 2/3 pyramidal neurons of male mice, we measured a marked reduction of mIPSC frequency immediately after RMS ($p_{L2/3,\ 0d} < 0.0001$, n = 5, *t*-test, Fig. 4B), that recovered to control levels following the 30-day rest period ($p_{L2/3,\ 30d} = 0.21$, n = 6, *t*-test, Fig. 4B). The amplitude of mIPSCs was indistinguishable between RMS and control mice (p-values > 0.4 at both time points, Fig. 4B). Similarly, we detected a reduction of mIPSC frequency in layer 2/3 pyramidal neurons of female mice that recovered to control levels after 30 days ($p_{L2/3,\ 0d} = 0.024$, n = 7, $p_{L2/3,\ 30d} = 0.63$, n = 6, *t*-test, Fig. 4C) and we saw no effect of RMS on the amplitude of inhibitory events (p-values > 0.4 at both time points, *t*-test, Fig. 4C). Two-way ANOVA revealed significant stress effect ($F_{1,\ 20} = 36.61$, $p < 0.0001$), significant effect of sex ($F_{1,\ 20} = 12.27$, $p = 0.0022$) and significant stress × sex interaction ($F_{1,\ 20} = 4.832$, $p = 0.0399$) immediately after RMS, while post hoc comparisons indicated significant sex differences in control ($p = 0.001$) but not in RMS ($p = 0.73$), and showed significant effect of RMS in both males ($p = 0.0001$) and females ($p = 0.015$). Following the recovery period, we found no main effects or interactions ($F_{1,21} < 3$, $p > 0.1$ for all comparisons). In layer 5 pyramidal neurons we measured a reduction of mIPSC frequency immediately after RMS in male mice ($p_{L5,\ 0d} = 0.038$, n = 5, *t*-test) that recovered to control level after 30 days ($p_{L5,\ 30d} = 0.17$, n = 5, *t*-test, Fig. 4E). We did not detect an effect of RMS on mIPSCs in layer 5 pyramidal neurons of female mice at either time point (all p-values > 0.1 at both time points, n = 6 at 0 days and 5 at 30 days, Fig. 4F). Two-way ANOVA revealed significant effect of stress ($F_{1,\ 19} = 4.568$, $p = 0.0458$) and sex ($F_{1,\ 19} = 5.545$, $p = 0.0294$) in layer 5 immediately after RMS but no effects following the 30-day recovery (stress: $F_{1,\ 17} = 3.070$, $p = 0.0977$, sex: $F_{1,\ 17} = 0.5142$, $p = 0.4831$).

These data suggest that in both sexes, prepubescent exposure to RMS causes a transient elimination of cortical inhibitory synapses, predominantly in superficial layers. However, we found a long-lasting reduction in hippocampal inhibitory synapse density in males but no effect in females.

Next, we wanted to determine the behavioral consequences of PPC excitatory synapse loss and recovery in both sexes. We have previously shown that in males, RMS-induced synapse loss in the PPC can be linked to decreased spontaneous alternation in the Y-maze (Libovner et al., 2020). Here we reproduced these results and found that an approximately 15% performance reduction in males persists over a 30-day rest period ($p_{0d} = 0.0003$, n = 25, $p_{30d} = 0.0016$, n = 21, *t*-test, Fig. 5A). In females, RMS exposure caused an 11% reduction in spontaneous alternation when measured immediately after RMS, but performance recovered following the 30-day rest ($p_{0d} = 0.0048$, n = 26, $p_{30d} = 0.43$, n = 14, *t*-test, Fig. 5A). Immediately after RMS, two-way ANOVA revealed main effect for stress ($F_{1,\ 104} = 23.55$, $p < 0.0001$) with multiple comparisons indicating no sex differences ($p > 0.3$ both in control and RMS) but significant effect of stress in both males ($p = 0.0002$) and females ($p = 0.001$). Following the 30-day recovery period, two-way ANOVA indicated main effect for stress ($F_{1,\ 67} = 7.158$, $p = 0.0094$), and post hoc comparisons showed significant sex difference in RMS mice ($p = 0.029$) but not in controls ($p > 0.99$) and marked stress effect in males ($p = 0.001$) but not in females ($p > 0.99$). These data suggest that sex differences in persistent excitatory synapse loss in the PPC are reflected in visuo-spatial working memory performance.

Decreased spontaneous alternation could be explained by altered motivation to explore or reduced mobility. To the contrary, we detected an increase in arm entries in both males and females immediately after RMS (males: $p_{0d} = 0.014$, females: $p_{0d} = 0.0015$, *t*-test, Fig. 5B). Two-way ANOVA revealing significant main effect for stress ($F_{1,\ 104} = 15.66$, $p = 0.0001$) but no sex differences $F_{1,\ 104} = 0.07408$, $p = 0.7860$). Following the 30-day rest period, there was no difference in arm entries in males but we saw a decrease in females (males: $p_{30d} = 0.55$, females: $p_{30d} = 0.036$ *t*-test, Fig. 5B). Sex differences emerged as the main effect in two-way ANOVA ($F_{1,\ 67} = 7.590$, $p = 0.0075$), with significant difference between males and females in the RMS condition ($p = 0.0031$) and significant difference between control and RMS in females ($p = 0.039$) but not in males ($p > 0.99$). These findings are not consistent with a loss of motivation or mobility after RMS, although a change in either of these metrics may have developed in females after the 30-day rest period, independent of spontaneous alternation performance.

The emergence of a depression-like phenotype could be an

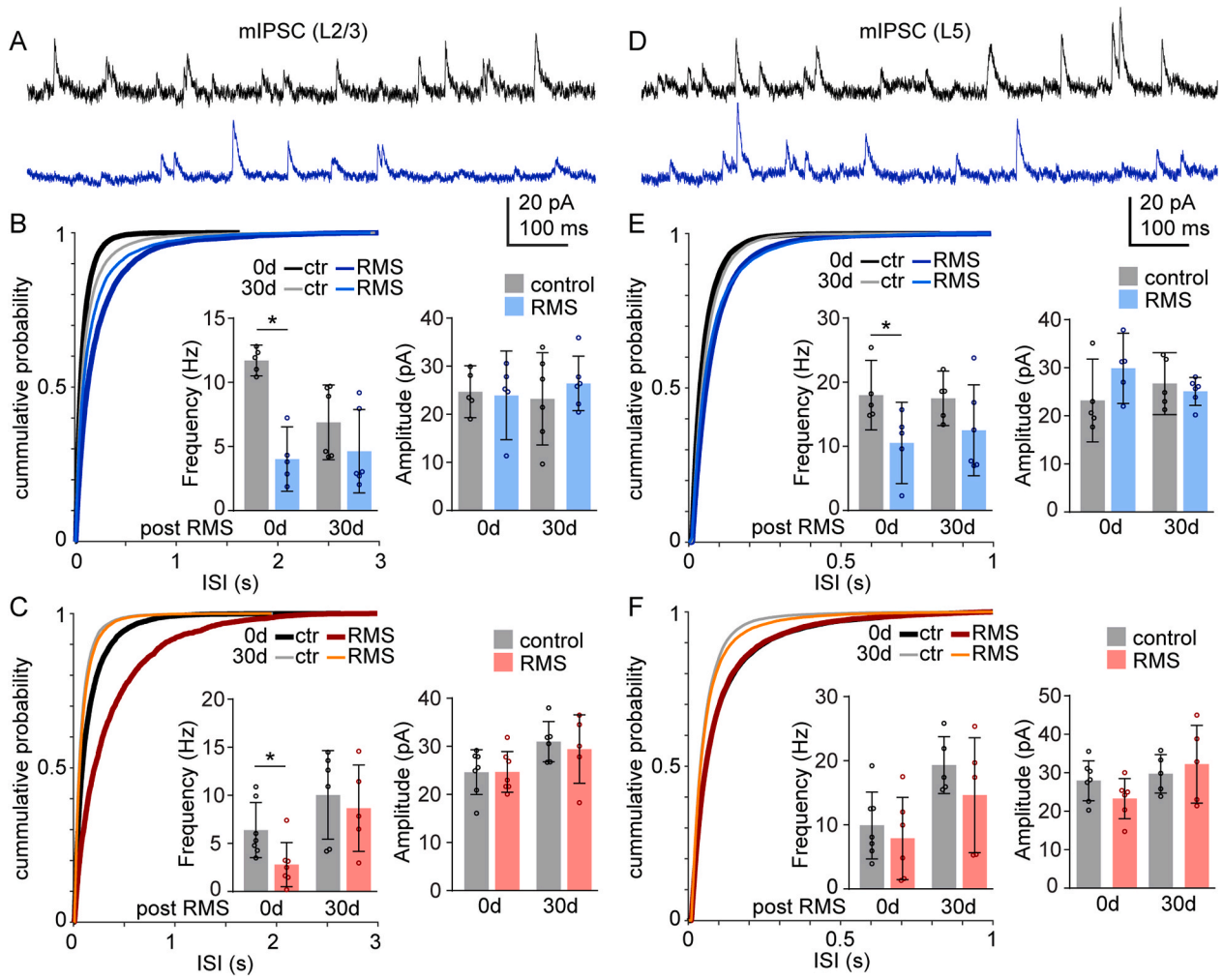

Fig. 4. RMS induces transient decrease of miniature IPSC frequency in layer 2/3 pyramidal neurons in both sexes. (**A**) Example miniature IPSC (mIPSC) recordings from layer 2/3 pyramidal neurons in the PPC of control (black) and RMS exposed (blue) mice. mISPC frequency and amplitude in layer 2/3 pyramidal neurons in control (gray) and post-RMS in (**B**) males (blue) and (**C**) females (red). (**D**) Example miniature EPSC (mEPSC) recordings from layer 5 pyramidal neurons in the PPC of control (black) and RMS exposed (blue) mice. mESPC frequency and amplitude in layer 5 pyramidal neurons in control (gray) and post-RMS in (**E**) males (blue) and (**F**) females (red). All bars represent mean with 95% confidence intervals, *: $p < 0.05$. Prepubescent RMS has persistent behavioral effects in males and a late developing phenotype in females. (For interpretation of the references to colour in this figure legend, the reader is referred to the Web version of this article.)

underlying driver of decreased spontaneous alternation in the Y-maze. To specifically test for learned helplessness, we used the forced swim paradigm. Contrary to our expectation, immediately after RMS male mice displayed a longer latency before the first bout of immobility while females showed no change (males: $p_{0d} = 0.0008$, n = 24, females: $p_{0d} = 0.12$, n = 36, *t*-test, Fig. 5C). Two-way ANOVA revealed significant main effect for stress ($F_{1, 119} = 13.13$ $p = 0.0004$) and significant stress × sex interaction ($F_{1, 119} = 7.422$, $p = 0.0074$) with post-hoc tests indicating sex differences in RMS mice ($p = 0.05$) but not in control ($p = 0.23$) and marked effect of RMS in males ($p = 0.0002$) but not in females ($p = 0.95$). Following the 30-day recovery period, this trend reversed and RMS exposed mice displayed shorter time to immobility in both sexes (males: $p_{30d} = 0.0005$, n = 20, females: $p_{30d} = 0.032$, n = 24, *t*-test, Fig. 5C). Two-way ANOVA indicated significant main effect for stress ($F_{1, 86} = 19.59$, $p < 0.0001$) with no sex difference ($p > 0.5$) but marked stress effect in both males ($p = 0.0005$) and females ($p = 0.039$). When comparing the time spent immobile immediately after RMS, two way ANOVA indicated a modest main effect for stress ($F_{1, 119} = 4.807$, $p = 0.0302$) although post hoc testing either within group or across conditions did not reveal significant stress effects or sex differences ($p > 0.1$ for all conditions, Fig. 5D). Following the 30-day rest period we found slightly reduced immobility time in females but no change in males (males: $p_{30d} = 0.17$, females: $p_{30d} = 0.043$, *t*-test, Fig. 5D). Two-way ANOVA indicated significant sex differences ($F_{1, 86} = 16.72$, $p < 0.0001$) and stress × sex interaction ($F_{1, 86} = 5.612$, $p = 0.02$) with post hoc testing revealing sex differences in control ($p = 0.0001$) and stress effect in females ($p = 0.038$). We have also tested whether prepubescent RMS exposure causes anhedonia-like behaviors but found control and RMS animals to have indistinguishable sucrose preference at both time points (all p-values > 0.15, n = 10 males and 18 females, *t*-test, Fig. 5D). These data suggest that reduced spontaneous alternation was not caused by a depression-like phenotype. However, we did observe learned helplessness in both sexes following the 30-day recovery period.

Spontaneous alternations may also be reduced in RMS mice due to heightened anxiety. To address this possibility, we used a light/dark box paradigm and measured latency to explore the bright side, total time spent in the bright chamber and the number of crosses between the chambers. Contrary to expectation, we found that immediately after RMS, male mice showed lower latency to enter the bright side, spent more time in the lit section and made more crosses between chambers than controls ($p_{latency, 0d} = 0.033$, $p_{time, 0d} < 0.0001$, $p_{cross, 0d} = 0.025$, n = 37, *t*-test, Fig. 6A, B, C). In females, all three metrics were indistinguishable from controls immediately after RMS (p-values > 0.2 for all metrics, n = 38, *t*-test, Fig. 6A, B, C). Two-way ANOVA tests indicated

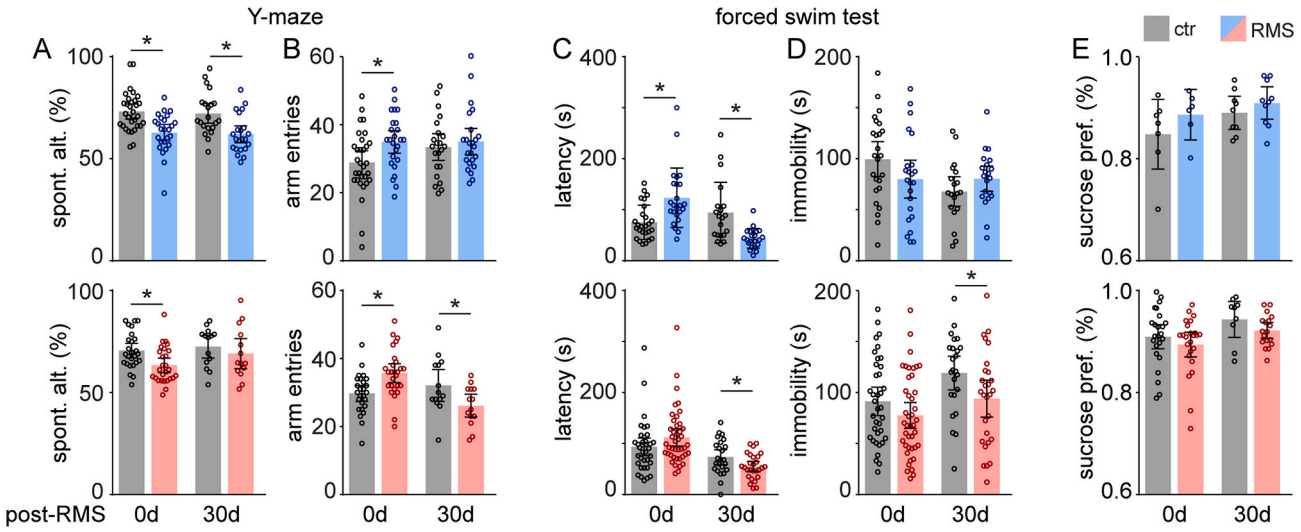

Fig. 5. RMS induces persistent impairment of visuo-spatial working memory in males. (**A**) Spontaneous alternation in the Y-maze in control (gray) and in RMS exposed males (blue) and females (red). (**B**) Number of arm entries in the Y-maze by control (gray) and in RMS exposed males (blue) and females (red). (**C**) Latency to first bout of immobility in forced swim in control (gray) and in RMS exposed males (blue) and females (red). (**D**) Total time spent immobile in the last 4 min of the forced swim test in control (gray) and in RMS exposed males (blue) and females (red). (**E**) Sucrose preference in control (gray) and in RMS exposed males (blue) and females (red). All bars represent mean with 95% confidence intervals, *: $p < 0.05$. (For interpretation of the references to colour in this figure legend, the reader is referred to the Web version of this article.)

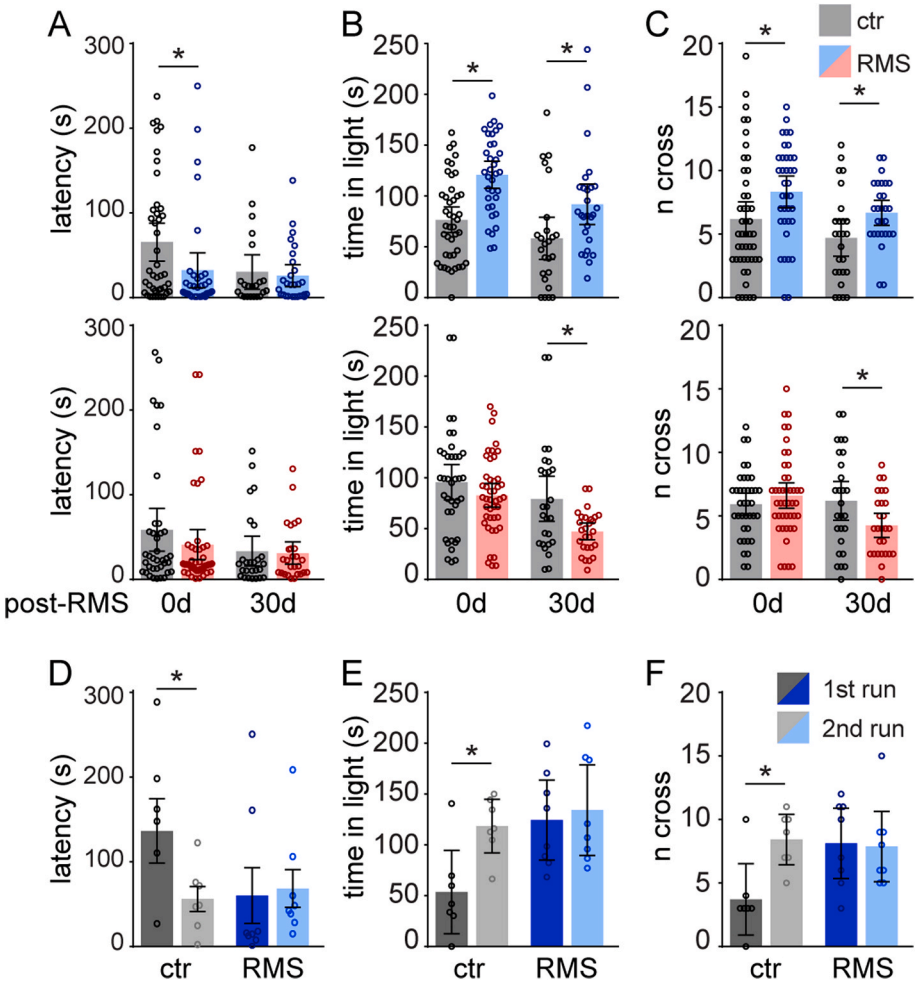

Fig. 6. RMS persistently reduces neophobia in males but induces late onset anxiety in females. (**A**) Latency to the first entry into the bright compartment in the light/dark box by controls (gray) and in RMS exposed males (blue) and females (red). (**B**) Time spent in the bright compartment of the light/dark box by controls (gray) and in RMS exposed males (blue) and females (red). (**C**) Number of crosses made between dark and light compartments by controls (gray) and in RMS exposed males (blue) and females (red). (**D**) Latency to first entry in to the bright compartment, (**E**) time spent in the bright, and (**F**) number of crosses made by controls on the first (dark gray) and second (light gray) exposure and by RMS exposed males on the first (dark blue) and second (light blue) to the light/dark box. All bars represent mean with 95% confidence intervals, *: $p < 0.05$. (For interpretation of the references to colour in this figure legend, the reader is referred to the Web version of this article.)

main stress effects in latency ($F_{1, 150} = 6.79$, $p = 0.0101$), time in light ($p = 0.023$), and number of crosses ($p = 0.012$), main sex effect in the number of crosses ($F_{1,150} = 4.18$, $p = 0.042$), and stress × sex interaction in time in light ($F_{1,150} = 17.7$, $p < 0.0001$). Post hoc testing revealed significant sex differences in RMS exposed mice for time in light ($p = 0.0002$) and number of crosses ($p = 0.024$), and significant stress effect in males for all three metrics ($p < 0.02$) but no effect in females ($p > 0.3$). Following the 30-day recovery period, males displayed similar behavior, measuring more time in light and a higher number of crosses ($p_{latency, 30d} = 0.69$, $p_{time, 30d} = 0.019$, $p_{cross, 30d} = 0.021$, $n = 26$, *t*-test, Fig. 6A, B, C). However, 30 days post-RMS, females spent less time in the bright compartment and crossed over fewer times than controls ($p_{latency, 30d} = 0.83$, $p_{time, 30d} = 0.0065$, $p_{cross, 30d} = 0.032$, $n = 27$, *t*-test, Fig. 6A, B, C). Two-way ANOVA tests found no main effects in latency but significant stress × sex interaction regarding time spent in the bright chamber ($F_{1, 101} = 13.47$, $p = 0.0004$), and in the number of crosses ($F_{1, 101} = 12$, $p = 0.0008$). In both measures, post hoc testing revealed significant sex difference in RMS mice ($p < 0.01$) and significant but opposing effect of RMS in males and females ($p < 0.05$). These data suggest that RMS exposure decreased anxiety in males. An alternative hypothesis was that in males, RMS reduced neophobia. To test this idea, we ran a small, separate cohort of mice in the light/dark box two consecutive times. A second exposure to the test markedly reduced the time to first entry and increased time spent in the bright compartment and the number of crosses in control males to the point where performance during the second exposure was indistinguishable from RMS exposed mice ($p_{ctr} = 0.021$, $p_{ctr} = 0.007$, $p_{ctr} = 0.0058$, $n = 7$, *t*-test, Fig. 6D, E, F). Two-way ANOVA tests indicated significant main effect for the number of exposures ($F_{1,24} > 4$, $p < 0.05$), and stress × number of exposures interaction ($F_{1,24} > 5$, $p < 0.05$) while post hoc testing revealed significant difference between first and second exposure in controls ($p < 0.05$) but not in RMS mice ($p > 0.99$) and significant difference between control and RMS animals during the first exposure ($p < 0.05$) but not during the second run ($p > 0.99$). These data suggest that RMS in males persistently reduces neophobia. On the contrary, we saw no such change in females but found a delayed development of increased neophobia or anxiety. This delayed effect of RMS in females was consistent with fewer arm entries in the Y-maze.

4. Discussion

Here we present evidence of sex differences in the long-term synaptic and behavioral effects of prepubescent stress. We found that exposure to multiple concurrent stressors eliminated excitatory synapses from deep layers of the PPC while diminishing inhibitory synapses in superficial layers in both sexes. This synapse loss coincided with impaired visuo-spatial working memory. However, following a 30-day recovery period, both synapse count and working memory performance recovered in female mice while the effects persisted in males. Conversely, females showed delayed expression of an anxiety-like behavioral phenotype, that was absent in males.

Our histological and electrophysiological analysis showed that prepubescent stress only eliminated excitatory synapses from deep layers of the PPC in both males and females. This data is in agreement with previous findings of reduced glutamatergic transmission in layer 5 pyramidal neurons in the medial prefrontal cortex (Yuen et al., 2012) and the lack of such effect in layer 2/3 of the anterior cingulate cortex (Ito et al., 2010). Our work extends previous results with a comparison across cortical layers and suggests that the immediate effect of prepubescent stress on excitatory transmission may be ubiquitous, at least in association areas of the rodent brain. These previous studies utilized repeated restraint, which is also an element of our RMS paradigm. Importantly, we compared the immediate effect of stress on excitatory synapses in both males and females and found similar patterns. Eiland and colleagues showed a comparable effect of adolescent stress in the two sexes (Eiland et al., 2012). A notable difference is that we did not see reduced PSD95 staining in the hippocampus of stressed females, although differing effects on dendritic complexity and synapse count may not be mutually exclusive. Notably, repeated social stress showed similar results in mid-adolescent male rats while spontaneous and miniature EPSC frequency was unaffected in females (Urban and Valentino, 2017).

In adult rodents, stress-induced changes in excitatory synapses are thought to recover after a short rest period (Conrad et al., 1999; Luine et al., 1994; Radley et al., 2005) while neonatal stresses tend to produce long-lasting effects (Goodman et al., 2019; Short and Baram, 2019; Dube et al., 2015; Bolton et al., 2017). The only study prior to ours examining synapse recovery following adolescent stress found lower than control synaptophysin immunoreactivity in the prefrontal cortex of male rats that persisted over a 3-week period (Leussis et al., 2008). Our histology and electrophysiology data reinforce these findings of persistent excitatory synapse loss in males. However, we show a remarkable recovery of PSD95 puncta density and mEPSC frequency in females, suggestive of marked sex differences in the recovery of excitatory transmission following prepubescent stress.

Contrary to excitatory synapses, we found that the effect of prepubescent stress on inhibitory connections was more prominent in superficial layers of the PPC in both sexes. There is only one other study that examined the impact of adolescent stress on inhibition, finding a similar reduction in layer 2/3 of the anterior cingulate cortex (Ito et al., 2010). There is more data available for adult rodents: immediately after one week of restraint, inhibitory synapses in the barrel cortex of mice appeared unaffected (Chen et al., 2018). Similarly, in adult rats, chronic mild stress did not cause a significant decrease of inhibitory synapses in the prefrontal cortex (Csabai et al., 2018).

There have been few attempts to understand the long-term effects of early life stress on cortical inhibition. Following maternal separation, one study found reduced inhibitory synapse density in the prefrontal cortex of adult rats (Ohta et al., 2020) while another study found increased spontaneous IPSCs frequency in mice (Franco et al., 2020). Both studies were limited to males. In contrast to excitatory transmission, we saw cortical inhibition recover to control levels following the 30-day rest period in both sexes. Overall, our findings suggest that inhibitory synapses are more sensitive to disruption in prepubescent animals than in adults, but the effect may not be as long-lasting as earlier interventions like neonatal stress.

In this study, we restricted electrophysiology recordings to miniature excitatory and inhibitory events in order to provide a physiological estimate of postsynaptic synapse density independent of immunostaining of PSD95 and Gephyrin. A caveat of this method is that it does not reveal potential changes in neuronal activity in the local microcircuit. Our previous work indicated a slight increase in pyramidal neuron excitability following prepubescent RMS (Libovner et al., 2020), which was in agreement with other groups that used restraint stress in rodents (Lee et al., 2011; Rosenkranz et al., 2010). Interestingly, repeated social stress in adolescent rats had the opposing effect on pyramidal neuron excitability (Urban and Valentino, 2017). These findings suggest that following restraint stress, there may be a disconnect between changes in intrinsic excitability and changes in synapse density in the local microcircuit. However, the effect on stress on postsynaptic events appears to be consistent between different paradigms.

We found that stress-induced changes in PPC synapses strongly correlated with a reduction of visuo-spatial working memory, measured by spontaneous alternation in the Y-maze. This paradigm has been shown to be sensitive to stress (Conrad et al., 1996, 2003) and to predominantly rely on intact PPC function (McNaughton et al., 1994; Rogers and Kesner, 2006; Save and Poucet, 2000; Spangler et al., 1994; Thomas and Weir, 1975). Our previous work indicates that a reduction of synaptic input from the visual system could play a significant role in the stress-induced impairment of this behavior (Libovner et al., 2020). These feed-forward sensory inputs are generally thought to target deeper cortical layers (Markov et al., 2014) suggesting that these

long-range afferents could make up a large proportion of the excitatory synapse loss in layers 5 and 6. Based on the canonical cortical microcircuit model (Douglas and Martin, 2004; Haeusler and Maass, 2007; Nelson, 2002), the majority of local excitation targeting deeper layers originates from layer 2/3. Our data suggests that the local circuit tries to compensate for the loss of long-range excitation in deeper layers by disinhibiting layer 2/3 pyramidal neurons, and thus enhancing the excitatory drive of layers 5 and 6. However, this compensatory mechanism does not appear to be sufficient to restore Y-maze performance, suggesting that processing long-range sensory inputs plays a critical role in the executive function of the PPC that cannot be substituted by homeostatic maintenance of the excitatory/inhibitory balance by the local microcircuit. To exhaustively test this hypothesis precise causal manipulation of these circuit elements during behavior will be necessary.

There are several reports on the immediate impact of adolescent stress on cognitive functions. These include reduced spatial memory in the Y-maze (Sterlemann et al., 2010) and object location (Stylianakis et al., 2018) tests, impaired temporal order recognition memory (Yuen et al., 2012) and diminished novel object recognition (Stylianakis et al., 2018; de Lima et al., 2017) while one study reported improved spatial learning (Isgor et al., 2004). All these studies exclusively focused on male rodents. Here we show that the immediate impact of prepubescent stress on visuo-spatial working memory is similar in male and female mice. A potential driving force underpinning decreased cognitive performance may be stress-induced depression or anxiety. There are indications of stress-induced depression in adolescent rodents, measured via reduced sucrose preference. Here, we did not see such effects in either males or females, although specific methodological considerations like the exact sucrose concentration or the length of stress exposure may be critical factors underlying these discrepancies (Phillips and Barr, 1997). Similarly to others (Eiland et al., 2012; de Lima et al., 2017), we found increased latency to immobility in forced swim, suggesting that immediately after stress exposure, prepubescent mice are not showing the classical learned helplessness phenotype. In the open field, stressed adolescent rodents showed enhanced locomotion (Ito et al., 2010; de Lima et al., 2017), which is in agreement with our detection of more frequent arm entries in the Y-maze in both sexes. When testing for anxiety phenotypes, several studies found increased light tolerance in the light/dark box test (Ito et al., 2010; de Lima et al., 2017; Ihne et al., 2012) suggesting reduced anxiety in stressed adolescent rodents. Our results indicated a marked sex difference in the light/dark box test immediately after RMS: while prepubescent males appeared to show reduced anxiety, the behavior of females was unaffected.

The long-term behavioral effects of adolescent stress are better studied than the underlying synaptic mechanisms. For example, spatial memory remained impaired in male rats for up to 6 weeks after repeated corticosterone administration (Stylianakis et al., 2018) and up to 3 weeks after chronic variable stress (Isgor et al., 2004). Our current study reinforces these findings showing long-term impairment of visuo-spatial working memory in stressed males but only transient impact on females. Interestingly, female rats exposed to repeated social stress displayed immediate cognitive impairment in a prefrontal cortex dependent task but their performance recovered by the time they reached adulthood while males showed the opposite pattern (Snyder et al., 2015; Snyder et al., 2015). Our results are in stark contrast with these findings, likely due to a number of key differences: we utilize a markedly different stress paradigm, study a different species and measure performance in a task linked to a different brain region. It would be interesting to bridge some of these differences for a better understanding of how different stress paradigms impact distinct brain regions and behaviors. In a recent study, adolescent mice exposed to chronic unpredictable stress followed by a 30-day rest period showed increased anxiety, measured by marble burying and time spent in the open arm of the elevated plus maze, decreased sucrose preference, and increased learned helplessness in the forced swim test (Yohn and Blendy, 2017). While this study examined the long-term effects of adolescent stress on both males and females, it only found significant sex differences in startle response (Yohn and Blendy, 2017). Our findings are in partial agreement; after recovery, we found decreased latency to immobility in forced swim indicating the delayed emergence of learned helplessness in both sexes. Furthermore, we found that females spent less time in the bright chamber of the light/dark box with fewer crossovers, suggesting increased anxiety. This idea is further supported by females executing fewer arm entries in the Y-maze after recovery, although it is somewhat contradicted by the increased mobility in forced swim. Conversely, males continued to exhibit reduced anxiety (more time in light and more crossovers in the light/dark box) even after the rest period. The interpretation of these behavioral results is somewhat complicated by the difficulty in separating potentially opposing stress effects on locomotion and anxiety. It is worth mentioning that we do not think that stress-induced synaptic changes in the PPC are related to the learned helplessness or anxiety phenotypes discussed here. Our goal in examining these behaviors was to provide a more complete picture of the potential driving forces underpinning the effect of RMS on spontaneous alternation in the Y-maze.

Notably, our stress paradigm specifically affects the prepubescent phase of adolescence (postnatal days 30–40). Ten days of stress exposure is relatively short, and certainly does not encompass the entire adolescent period in mice (postnatal day 21–59). It is to be explored in future works whether longer stress exposure would result in non-reversible effects and possibly neutralize or exaggerate the observed sex-differences. It must also be noted that the effects of stress on post-puberty females are likely influenced by the estrus cycle (Romeo et al., 2003), a variable we did not control for in this study.

CRediT authorship contribution statement

Mona Fariborzi: Conceptualization, Investigation, Formal analysis, Writing - original draft. **Soo Bin Park:** Investigation, Formal analysis, Writing - review & editing. **Ali Ozgur:** Investigation, Formal analysis, Writing - review & editing. **Gyorgy Lur:** Conceptualization, Investigation, Formal analysis, Writing - original draft, Funding acquisition.

Declaration of competing interest

The authors declare no conflict of interest.

Acknowledgements

We thank Mikko Oijala for his assistance in developing the software package to analyze miniature synaptic events. These studies were funded by the Whitehall Foundation: 2018-12-09 (GL), and the NIHM: R01MH123686 (GL) and the UROP program at UCI (MF).

References

Andersen, S.L., 2003. Trajectories of brain development: point of vulnerability or window of opportunity? Neurosci. Biobehav. Rev. 27 (1–2), 3–18.
Ankri, L., Yarom, Y., Uusisaari, M.Y., 2014. Slice it hot: acute adult brain slicing in physiological temperature. JoVE (92) p. e52068.
Bangasser, D.A., Wiersielis, K.R., 2018. Sex differences in stress responses: a critical role for corticotropin-releasing factor. Athens Hormones (Basel) 17 (1), 5–13.
Bangasser, D.A., et al., 2010. Sex differences in corticotropin-releasing factor receptor signaling and trafficking: potential role in female vulnerability to stress-related psychopathology. Mol. Psychiatr. 15 (9), 877, 896-904.
Beck, K.D., Luine, V.N., 2002. Sex differences in behavioral and neurochemical profiles after chronic stress: role of housing conditions. Physiol. Behav. 75 (5), 661–673.
Blakemore, S.J., Choudhury, S., 2006. Development of the adolescent brain: implications for executive function and social cognition. JCPP (J. Child Psychol. Psychiatry) 47 (3–4), 296–312.
Boden, J.M., Horwood, L.J., Fergusson, D.M., 2007. Exposure to childhood sexual and physical abuse and subsequent educational achievement outcomes. Child Abuse Negl. 31 (10), 1101–1114.
Bolton, J.L., et al., 2017. New insights into early-life stress and behavioral outcomes. Curr. Opin. Behav. Sci. 14, 133–139.

Bremner, J.D., et al., 1999a. Neural correlates of exposure to traumatic pictures and sound in Vietnam combat veterans with and without posttraumatic stress disorder: a positron emission tomography study. Biol. Psychiatr. 45 (7), 806–816.
Bremner, J.D., et al., 1999b. Neural correlates of memories of childhood sexual abuse in women with and without posttraumatic stress disorder. Am. J. Psychiatr. 156 (11), 1787–1795.
Bremner, J.D., et al., 2004. Neural correlates of the classic color and emotional stroop in women with abuse-related posttraumatic stress disorder. Biol. Psychiatr. 55 (6), 612–620.
Chen, Y., et al., 2000. Immunocytochemical distribution of corticotropin-releasing hormone receptor type-1 (CRF(1))-like immunoreactivity in the mouse brain: light microscopy analysis using an antibody directed against the C-terminus. J. Comp. Neurol. 420 (3), 305–323.
Chen, Y., et al., 2008. Rapid loss of dendritic spines after stress involves derangement of spine dynamics by corticotropin-releasing hormone. J. Neurosci. 28 (11), 2903–2911.
Chen, C.C., et al., 2018. Selective activation of parvalbumin interneurons prevents stress-induced synapse loss and perceptual defects. Mol. Psychiatr. 23 (7), 1614–1625.
Clements, J.D., Bekkers, J.M., 1997. Detection of spontaneous synaptic events with an optimally scaled template. Biophys. J. 73 (1), 220–229.
Conrad, C.D., et al., 1996. Chronic stress impairs rat spatial memory on the Y maze, and this effect is blocked by tianeptine pretreatment. Behav. Neurosci. 110 (6), 1321–1334.
Conrad, C.D., et al., 1999. Repeated restraint stress facilitates fear conditioning independently of causing hippocampal CA3 dendritic atrophy. Behav. Neurosci. 113 (5), 902–913.
Conrad, C.D., et al., 2003. Sex differences in spatial and non-spatial Y-maze performance after chronic stress. Neurobiol. Learn. Mem. 79 (1), 32–40.
Csabai, D., Wiborg, O., Czeh, B., 2018. Reduced synapse and axon numbers in the prefrontal cortex of rats subjected to a chronic stress model for depression. Front. Cell. Neurosci. 12, 24.
Dahl, R.E., 2004. Adolescent brain development: a period of vulnerabilities and opportunities. Keynote address. Ann. N Y Acad. Sci. 1021, 1–22.
de Lima, A.P., et al., 2017. Long-lasting monoaminergic and behavioral dysfunctions in a mice model of socio-environmental stress during adolescence. Behav. Brain Res. 317, 132–140.
Douglas, R.J., Martin, K.A., 2004. Neuronal circuits of the neocortex. Annu. Rev. Neurosci. 27, 419–451.
Dube, C.M., et al., 2015. Hyper-excitability and epilepsy generated by chronic early-life stress. Neurobiol. Stress 2, 10–19.
Dunkley, B.T., et al., 2015. Theta, mental flexibility, and post-traumatic stress disorder: connecting in the parietal cortex. PLoS One (4), 10 p. e0123541.
Eiland, L., Romeo, R.D., 2013. Stress and the developing adolescent brain. Neuroscience 249, 162–171.
Eiland, L., et al., 2012. Chronic juvenile stress produces corticolimbic dendritic architectural remodeling and modulates emotional behavior in male and female rats. Psychoneuroendocrinology 37 (1), 39–47.
Franco, L.O., et al., 2020. Social subordination induced by early life adversity rewires inhibitory control of the prefrontal cortex via enhanced Npy1r signaling. Neuropsychopharmacology 45 (9), 1438–1447.
Giedd, J.N., Rapoport, J.L., 2010. *Structural MRI of pediatric brain development: what have we learned and where are we going?* Neuron, 67 (5), 728–734.
Goodman, J.B., Freeman, E.E., Chalmers, K.A., 2019. The relationship between early life stress and working memory in adulthood: a systematic review and meta-analysis. Memory 27 (6), 868–880.
Gould, F., et al., 2012. The effects of child abuse and neglect on cognitive functioning in adulthood. J. Psychiatr. Res. 46 (4), 500–506.
Grafe, L.A., et al., 2017. Orexins mediate sex differences in the stress response and in cognitive flexibility. Biol. Psychiatr. 81 (8), 683–692.
Haeusler, S., Maass, W., 2007. *A statistical analysis of information-processing properties of lamina-specific cortical microcircuit models.* Cereb Cortex, 17 (1), 149–162.
Hart, H., et al., 2017. Reduced functional connectivity of fronto-parietal sustained attention networks in severe childhood abuse. PloS One (11), 12.
Hokenson, R.E., Oijala, M., Short, A.K., Bolton, J.L., Chen, Y., Molet, J., Maras, P.M., Baram, T.Z., Lur, G., 2020. Multiple simultaneous acute stresses in mice: single or repeated induction. Bio-Protocol 10 (15), 33699.
Ihne, J.L., et al., 2012. Pharmacological modulation of stress-induced behavioral changes in the light/dark exploration test in male C57BL/6J mice. Neuropharmacology 62 (1), 464–473.
Isgor, C., et al., 2004. Delayed effects of chronic variable stress during peripubertal-juvenile period on hippocampal morphology and on cognitive and stress axis functions in rats. Hippocampus 14 (5), 636–648.
Ito, H., et al., 2010. Chronic stress enhances synaptic plasticity due to disinhibition in the anterior cingulate cortex and induces hyper-locomotion in mice. Neuropharmacology 58 (4–5), 746–757.
Kitay, J.I., 1961. Sex differences in adrenal cortical secretion in the rat. Endocrinology 68, 818–824.
Kitraki, E., et al., 2004. Gender-dependent alterations in corticosteroid receptor status and spatial performance following 21 days of restraint stress. Neuroscience 125 (1), 47–55.
Kolassa, I.T., et al., 2007. Altered oscillatory brain dynamics after repeated traumatic stress. BMC Psychiatr. 7, 56.
Lamprecht, M.R., Sabatini, D.M., Carpenter, A.E., 2007. *CellProfiler: free, versatile software for automated biological image analysis.* Biotechniques, 42 (1), 71–75.
Lanius, R.A., et al., 2002. Brain activation during script-driven imagery induced dissociative responses in PTSD: a functional magnetic resonance imaging investigation. Biol. Psychiatr. 52 (4), 305–311.
Lee, Y.A., et al., 2011. Dorsal-ventral distinction of chronic stress-induced electrophysiological alterations in the rat medial prefrontal cortex. Neuroscience 183, 108–120.
Lenroot, R.K., Giedd, J.N., 2006. Brain development in children and adolescents: insights from anatomical magnetic resonance imaging. Neurosci. Biobehav. Rev. 30 (6), 718–729.
Leussis, M.P., et al., 2008. The enduring effects of an adolescent social stressor on synaptic density, part II: poststress reversal of synaptic loss in the cortex by adinazolam and MK-801. Synapse 62 (3), 185–192.
Libovner, Y., et al., 2020. Repeated exposure to multiple concurrent stresses induce circuit specific loss of inputs to the posterior parietal cortex. J. Neurosci. 40 (9), 1849–1861.
Liston, C., et al., 2006. Stress-induced alterations in prefrontal cortical dendritic morphology predict selective impairments in perceptual attentional set-shifting. J. Neurosci. 26 (30), 7870–7874.
Liston, C., McEwen, B.S., Casey, B.J., 2009. Psychosocial stress reversibly disrupts prefrontal processing and attentional control. Proceedings of the National Academy of Sciences of the United States of America, 106 (3), 912–917.
Luine, V., et al., 1994. Repeated stress causes reversible impairments of spatial memory performance. Brain Res. 639 (1), 167–170.
Luine, V., et al., 2017. Sex differences in chronic stress effects on cognition in rodents. Pharmacol. Biochem. Behav. 152, 13–19.
Magarinos, A.M., McEwen, B.S., 1995. Stress-induced atrophy of apical dendrites of hippocampal CA3c neurons: involvement of glucocorticoid secretion and excitatory amino acid receptors. Neuroscience 69 (1), 89–98.
Maras, P.M., et al., 2014. Preferential loss of dorsal-hippocampus synapses underlies memory impairments provoked by short, multi-modal stress. Mol. Psychiatr. 19 (7), 745.
Markov, N.T., et al., 2014. Anatomy of hierarchy: feedforward and feedback pathways in macaque visual cortex. Journal of comparative neurology, 522 (1), 225–259.
McEwen, B.S., 1999. Stress and hippocampal plasticity. Annu. Rev. Neurosci. 22, 105–122.
McEwen, B.S., 2014. Sex, stress and the brain: interactive actions of hormones on the developing and adult brain. Climacteric 18–25, 17 Suppl 2.
McEwen, B.S., Milner, T.A., 2007. *Hippocampal formation: shedding light on the influence of sex and stress on the brain.* Brain Res Rev, 55 (2), 343–355.
McNaughton, B.L., et al., 1994. Cortical representation of motion during unrestrained spatial navigation in the rat. Cerebr. Cortex 4 (1), 27–39.
McQuin, C., et al., 2018. CellProfiler 3.0: next-generation image processing for biology. PLoS Biol (7), 16 p. e2005970.
Mengler, L., et al., 2014. Brain maturation of the adolescent rat cortex and striatum: changes in volume and myelination. Neuroimage 84, 35–44.
Miedel, C.J., et al., 2017. Assessment of spontaneous alternation, novel object recognition and limb clasping in transgenic mouse models of amyloid-beta and tau neuropathology. JoVE (123).
Nelson, S., 2002. *Cortical microcircuits: diverse or canonical?* Neuron, 36 (1), 19–27.
Ohta, K.I., et al., 2020. The effects of early life stress on the excitatory/inhibitory balance of the medial prefrontal cortex. Behav. Brain Res. 379, 112306.
Ortiz, J.B., et al., 2015. Sex-specific impairment and recovery of spatial learning following the end of chronic unpredictable restraint stress: potential relevance of limbic GAD. Behav. Brain Res. 282, 176–184.
Phillips, A.G., Barr, A.M., 1997. Effects of chronic mild stress on motivation for sucrose: mixed messages. Psychopharmacology (Berl.) 134 (4), 361–366 discussion 371-7.
Piefke, M., et al., 2007. The neurofunctional mechanisms of traumatic and non-traumatic memory in patients with acute PTSD following accident trauma. Neurocase 13 (5), 342–357.
Radley, J.J., et al., 2005. Reversibility of apical dendritic retraction in the rat medial prefrontal cortex following repeated stress. Exp. Neurol. 196 (1), 199–203.
Radley, J.J., et al., 2006. Repeated stress induces dendritic spine loss in the rat medial prefrontal cortex. Cerebr. Cortex 16 (3), 313–320.
Rogers, J.L., Kesner, R.P., 2006. Lesions of the dorsal hippocampus or parietal cortex differentially affect spatial information processing. Behav. Neurosci. 120 (4), 852–860.
Romeo, R.D., 2013. *The teenage brain: the stress Response and the adolescent brain.* Curr dir psychol sci, 22 (2), 140–145.
Romeo, R.D., et al., 2003. Anxiety and fear behaviors in adult male and female C57BL/6 mice are modulated by maternal separation. Horm. Behav. 43 (5), 561–567.
Romeo, R.D., et al., 2006. Stress history and pubertal development interact to shape hypothalamic-pituitary-adrenal axis plasticity. Endocrinology 147 (4), 1664–1674.
Rosenkranz, J.A., Venheim, E.R., Padival, M., 2010. Chronic stress causes amygdala hyperexcitability in rodents. Biol. Psychiatr. 67 (12), 1128–1136.
Salvatore, M., et al., 2018. Sex differences in circuits activated by corticotropin releasing factor in rats. Horm. Behav. 97, 145–153.
Sanchez, M.M., et al., 2000. Distribution of corticosteroid receptors in the rhesus brain: relative absence of glucocorticoid receptors in the hippocampal formation. J. Neurosci. 20 (12), 4657–4668.
Save, E., Poucet, B., 2000. Hippocampal-parietal cortical interactions in spatial cognition. Hippocampus 10 (4), 491–499.
Shansky, R.M., et al., 2006. The effects of sex and hormonal status on restraint-stress-induced working memory impairment. Behav. Brain Funct. 2, 8.
Shomstein, S., 2012. Cognitive functions of the posterior parietal cortex: top-down and bottom-up attentional control. Front. Integr. Neurosci. 6, 38.

Short, A.K., Baram, T.Z., 2019. Early-life adversity and neurological disease: age-old questions and novel answers. Nat. Rev. Neurol. 15 (11), 657–669.
Snyder, K., et al., 2015. The impact of social stress during adolescence or adulthood and coping strategy on cognitive function of female rats. Behav. Brain Res. 286, 175–183.
Snyder, K.P., Barry, M., Valentino, R.J., 2015. Cognitive impact of social stress and coping strategy throughout development. Psychopharmacology (Berl.) 232 (1), 185–195.
Soares, J.M., et al., 2012. Stress-induced changes in human decision-making are reversible. Transl. Psychiatry 2 p. e131.
Sousa, N., et al., 2000. Reorganization of the morphology of hippocampal neurites and synapses after stress-induced damage correlates with behavioral improvement. Neuroscience 97 (2), 253–266.
Spangler, E.L., et al., 1994. *Thrombosis of parietal, but not striate, cortex impairs acquisition of a 14-unit T-maze in the rat.* Physiol Behav, 56 (1), 95–101.
Spear, L.P., 2000. The adolescent brain and age-related behavioral manifestations. Neurosci. Biobehav. Rev. 24 (4), 417–463.
Stark, E., et al., 1975. Corticosteroid receptors in the central nervous system of the rat. Acta Phys. Acad. Sci. Hungar. 46 (2), 115–124.
Sterlemann, V., et al., 2010. Chronic social stress during adolescence induces cognitive impairment in aged mice. Hippocampus 20 (4), 540–549.
Stylianakis, A.A., et al., 2018. Differences in the persistence of spatial memory deficits induced by a chronic stressor in adolescents compared to juveniles. Dev. Psychobiol. 60 (7), 805–813.
Thomas, R.K., Weir, V.K., 1975. Effects of lesions in frontal or posterior association cortex of rats on maze iii. Physiol. Psychol. 3 (3), 210–214.
Ting, J.T., et al., 2014. Acute brain slice methods for adult and aging animals: application of targeted patch clamp analysis and optogenetics. Methods Mol. Biol. 1183, 221–242.
Urban, K.R., Valentino, R.J., 2017. *Age- and sex-dependent Impact of repeated social Stress on Intrinsic and synaptic Excitability of the rat prefrontal cortex.* Cereb cortex, 27 (1), 244–253.
Urban, K.R., et al., 2019. Age- and sex-dependent impact of repeated social stress on morphology of rat prefrontal cortex pyramidal neurons. Neurobiol. Stress 10, 100165.
Yohn, N.L., Blendy, J.A., 2017. Adolescent chronic unpredictable stress exposure is a sensitive window for long-term changes in adult behavior in mice. Neuropsychopharmacology 42 (8), 1670–1678.
Yuen, E.Y., et al., 2012. Repeated stress causes cognitive impairment by suppressing glutamate receptor expression and function in prefrontal cortex. Neuron 73 (5), 962–977.
Zoratto, F., et al., 2018. Inside the developing brain to understand teen behavior from rat models: metabolic, structural, and functional-connectivity alterations among limbic structures across three pre-adolescent stages. Front. Behav. Neurosci. 12, 208.